Application of Terrestrial Laser Scanner to the Assessment of the Evolution of Diachronic Landslides

José A. Palenzuela, Clemente Irigaray, Jorge D. Jiménez-Perálvarez, and José Chacón

Abstract

During the diachronic evolution of landslides, slope-morphology changes may be detected and assessed by using high-resolution digital models. Slope deformation is detected by scanning sequences over a given time period. This paper presents the results found combining TLS digital models and Global Navigation Satellite Systems in the detection and assessment of reactivations and differential displacements of two slides located at the SW of Sierra Nevada (Spain) between 2008 and 2010. In the first landslide a maximum downward movement of 1.2 m at the top was measured, whereas below the middle part of the mass, 1.3 m of maximum advance was established with a maximum displacement gradient of 1.04 m/year. In the second landslide, downward displacements with gradients between 0.32 m and 0.56 m/year were found, corresponding to rupture movements in incipient to initial stages of evolution. The combined use of TLS and GNSS enabled a quantification and mapping of complementary terrain features which are considered useful in forecasting further activity and slope evolution of these landslides. The high resolution and accuracy of the techniques applied offer broad possibilities in the spatial location of the slope movement and also in forecasting its diachronic activity.

Keywords

Landslide • Activity • Displacement • TLS • ICP • GIS

Introduction

For the prevention of landslides, spatial data are useful in preparing susceptibility maps; nevertheless, in the case of hazard and risk maps, temporal data and information concerning the destructive capacity of landslides are also necessary (Chacón et al. 2006). For the analysis of the diachronic evolution of slope movements (Chacón et al. 2010) the degree of activity and development, velocity, volume of displaced masses, and the morphological evolution of the slope are quantified, including the scarps and zones of reduction and accumulation of displaced masses (IAEG 1993, 1995; Cruden and Varnes 1996; Fernández et al. 2003; Corominas and Moya 2008; Fell et al. 2008; Fernández et al. 2009).

One of the most powerful tools for monitoring, characterizing, and quantifying the relief evolution, including landslides, is Terrestrial Laser Scanning (TLS) (Teza et al. 2008; Dunning et al. 2009; Abellán et al. 2010; Dunning et al. 2010). This technique provides a high-resolution cloud of points measured in time-of-flight on the slope surface by using an infrared pulse emission in a known direction. The three-dimensional variation of the slope features are detected and quantified by a treatment and analysis of sequences of data gathered over a given time (Lim et al. 2005; Rosser et al. 2005; Oppikofer et al. 2009).

This technique has been applied to the detection of slope deformations prior to rockfall (Abellán et al. 2010), the determination of amount of slope displacement (Teza et al. 2007;

J.A. Palenzuela (✉) • C. Irigaray • J.D. Jiménez-Perálvarez • J. Chacón
Department of Civil Engineering, University of Granada, Avda. Fuentenueva s/n, Granada, Spain

C. Margottini et al. (eds.), *Landslide Science and Practice*, Vol. 2,
DOI 10.1007/978-3-642-31445-2_68, © Springer-Verlag Berlin Heidelberg 2013

Oppikofer et al. 2009), and the gathering of geometrical and morphological features, as well as other objectives (Dunning et al. 2009, 2010).

In this paper the methodology and results on combining TLS and GNSS (Global Navigation Satellite Systems) were applied to detect and assess morphological slope features, movements, reactivations, and differential displacements in the landslides of Almegíjar and Borincho, settled in the SE of Sierra Nevada (Granada, southern Spain), representative of the slope movements in a sector with high landslide susceptibility extensively affected by slope-instability processes (Chacón et al. 2006; Fernández et al. 2009; Jiménez-Perálvarez et al. 2009). In Almegíjar landslide, previous results, by means of photogrammetry techniques (Fernández et al. 2011), suggest non-uniform sliding activity with a diachroneity duration scale of VIII (Chacón et al. 2010) corresponding to slope movements with irregular activity, alternating phases of low activity with reactivations, due mainly to heavy rainfall.

Study Zone

The Almegíjar and Borincho planar slides are settled in the Alpujarride Complex of the Betic Cordillera (Fig. 1), a major tectonic unit composed of widespread phyllite, calcareous schist, and marble of Late Permian to Triassic outcropping from the NE to SW of southern Spain along its Mediterranean border. Both are located in Granada province, on the SW margin of Sierra Nevada in the northern part of the Guadalfeo River basin, in a hilly to mountainous region heavily divided by river channels and abundant landslides (Jiménez-Perálvarez et al. 2009). These two slides affect slopes of between 40 % and 60 % and a rock massif of low strength and very low permeability composed mainly of phyllite, both conditions favouring the instability process.

Methods and Materials

In this research, a TLS Riegl® 420 i system (Riegl 2011) was used for remote sensing by Laser Imaging Detection and Ranging (LIDAR), complemented by a distance explorer of the type Time of Flight (TOF), providing data on distances as well as spherical and Cartesian scales of the measurement positioning in the scanning system. This technology supplies high-density measuring (thousand points per second) with centimetric precision and accuracy, thus permitting the exploration of the entire scanned surface and the detection of small-sized features.

The error or reliability of the measure positioning in a plane perpendicular to the scanning laser beam is determined by the distance to the observation target and the angular divergence of the laser beam (Lichti and Jamtsho 2006; Riegl 2011), which reaches 0.25 mrad/50 m. The linear error in the distance to the target measured reaches 1 cm plus 20 ppm times the range. In the slopes studied, with observation distances of less than 600 m, the distance errors measured were less than 22 mm, and the dispersion in the position of the collimator point less than 125 mm.

Besides distance measurements, a direct geo-referencing in absolute coordinates was implemented, following the static positioning method with GNSS (GPS + GLONAS) of millimetric accuracy, by the correction of measurements gained from two permanent reference surveying stations with pinpointed with exact geodetic coordinates. In this way, minimum accuracies, related to the global position, of 11 and 17 mm were achieved for the horizontal and vertical components, respectively, for the Almegíjar slide, and 37 and 51 mm for the Borincho slide.

The methodology involved the following stages:

Planning

In this stage the landslides to be studied are selected, and the timing and positioning of scanning are determined:

Selection of Landslides Targets

This is based mainly on a review of geomorphological and landslide-susceptibility maps of the region (Jiménez-Perálvarez et al. 2010), where information concerning the activity and potential development of landslides are available.

Determination of Scanning Points

The location of correct scanning points permits measurements to be established over most of the study target, minimising the accumulative error during the alignment of the different scanning and shadow or hole zones.

Scanning Timing

For the Almegíjar slide, three scans were made, on 15/07/2008, 10/03/2009, 11/06/2010. This included an extraordinarily rainy period between the latter two dates, corresponding to the December 2009–March 2010 term, with a record of 500 mm of rain and an average value for this period of 250 mm.

For the Borincho slide, two scannings were made: in 12/03/2009 and 15/06/2010, also including the wet period 2009–2010.

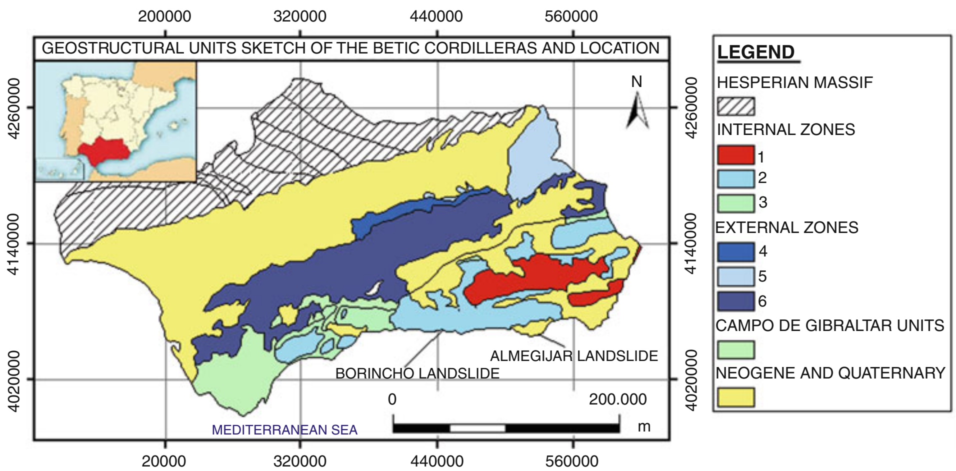

Fig. 1 Tectonic sketch of major geo-structural units of the Betic Cordillera, and setting of the two study zones. (*1* Nevado-Filábride Complex, *2* Alpujárride Complex, *3* Maláguide and Dorsale units, *4* Intermediate units, *5* Prebetic zone, *6* Subbetic and Penibetic zones)

Field Surveying Research

Setting of Control Target Points on Field Sites (GCPs)

With the morphological boundaries of the slide taken into account, external and internal GCPs were used as scattered and misaligned as possible, in order to achieve the main objective of this scanning, which was to find a good correlation for the tie points in the resulting scanned cloud of points. These target control points were made with highly reflective material clearly differentiated from other points in the scanned cloud. In order to facilitate a merging of data sets from different dates, without including those affected by displacements during the time interval, points in the external parts of the slide were intended to acquire a permanent character, despite the difficulties or factors this implies. On the other hand, the alignment of data achieved on the same date may also be supported by the internal tie points. The GCPs were installed seeking the highest intervisibility between them and with the other scanning positions in each study zone.

TLS and GNSS Data Acquisition

In this stage TLS was installed in each scanner coordinate system (SOCSi), with a calibrated GNSS receiver to determine its position. For a direct geo-referencing in the global coordinate system (GLCS), a back-sighting point or BS point was installed with registered geodetic coordinates.

Data Processing

This is the most important stage of the methodology, which includes the preparation of the raw data, the global cloud-point merging, its accuracy and that of the final terrain model depending greatly on the quality of the alignments and adjustments between the different data sets. Finally, it concludes with the information comparison and interpretation.

Reduction of the Point Cloud

The implementing of a filter with Octant Tree Structure (OCTREE) is to minimize the spread of each temporal data set, and to attain a file size manageable by the available computer software and hardware, maintaining the representativeness of the actual surface by the centres of gravity of cubes with a minimum side length of 0.1 mm for the centimetre resolution reached during the site scanning.

Alignment

This is a registration or merging between each specific system for each scanning position ($SOCS_i$) and one of them chosen as Project Control System (PRCS). In a further step, this system is transformed into the global coordinate system (GLCS) by means of direct geo-referencing.

The procedure is carried out by assigning tie points manually (Coarse registration), or automatically if a GCPs (Fine registration) is available.

In the Almegíjar slide, control points (GCPs) were available for all the scanning positions, except for a case in which some difficulties were encountered in detecting a sufficient number of tie points for an automated alignment. Except in that position, where the standard deviation between the tie-point positions of a data set and the PRCS was of 47 cm, the value for the other aligned data sets was between 1 and 7.7 cm.

In the Borincho slide, only the second data-acquisition control points were available, and therefore the cloud of points corresponding to 12/3/2009 was aligned by coarse registration until the GCPs previously installed permitted an automated alignment. In the first case of coarse registration the standard deviation of the values reached between 12 and 20 cm, until in the automated registration the value was 0.8 cm.

Multistation Adjustment (MSA)

When errors in the previous stage over the transform of coordinates reached values of more than 2.5 cm, the parameters were improved in this matrix running the SOCSs multistation adjustment until the errors were below that value. This procedure is generally based on the Iterative Closest Point (ICP), an iterative supervised adjustment by applying an algorithm implemented by most software packages for 3D treatment, such as the Riscan Pro software (Riegl 2010), applied in this research.

The ICP algorithm calculates not only the distance between artificial targets, tie points or tie objects created with a previous filtering of plane surfaces, but also the angles between the normal vectors of the tie objects corresponding to each data set, trying to minimize these values in each iteration.

By means of this adjustment a final standard deviation between 0.5 and 2.5 cm resulted for the Almegíjar slide and between 0.8 and 2.2 cm for the Borincho slide.

Filtering of Features not Acceptable for the Analysis

Consecutively, trees, shrubs, and taller vegetation constituting noise in the analysis of topographic changes of the ground surface are removed. A semiautomatic method is used, consisting of the elimination of "floating points" on site of a metric-width section (2–20 m) which is progressively displaced along the entire scanned surface (Riegl 2010).

Triangulation

Once filtered, all survey data, a mathematical model of reference for comparison of temporal data is built up, creating a triangular irregular network (TIN) using the Delaunay triangulation algorithm.

Information Analysis and Interpretation of Results

At this stage, we have used the Risca Pro software, which provides tools for comparative analysis of multi-temporal data. Given the difficulty of defining a reference plane for calculating orthogonal displacements resulting from the high irregularity of the site topography, a variant of the Surface Comparison algorithm was adopted for assessing the minimum distance (D_i) from the selected surface points (q_i) to the average plane of the triangles adjacent to the nearest point (p_i) of the reference surface in the direction of its normal vector. Starting with these orthogonal displacements to the average plane, the triangles adjacent to q_i were classified depending of their values, resulting in a distribution of the minimum displacement undergone by the modelled surfaces

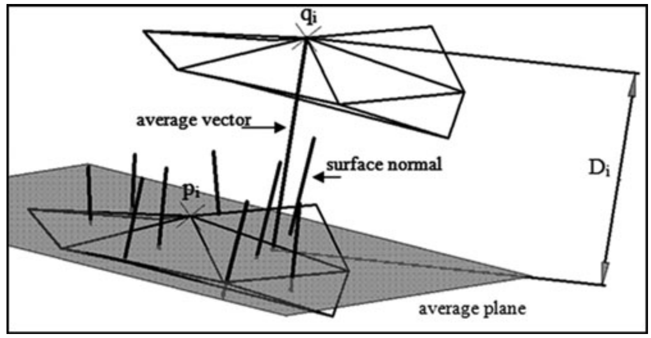

Fig. 2 Determination of distance Di

in each temporal interval. This classification was performed in a supervised way considering the detection and quantification of slope features related to the sliding. The values found were differentiated between positive and negative, when q_i fell above or below the average plane, respectively (Fig. 2). The negative values were interpreted as areas of relief loss either by erosion, subsidence, scarp back warding, etc., whereas to those zones classified with positive values corresponded to depositional zones, slope mass advance, debris accumulation, etc..

Results

The slope features and changes detected following this methodology are described as follows:

Geomorphological Evolution of the Almegíjar Slide

- Period 7/2008–3/2009 (Fig. 3a): only topographical variations derived from erosive processes with values in the range −0.15 to 0.50 m with reference to a TIN from July 2008 were detected. The highest erosion concentrates in the highest part of the scarp, whereas the thickening of the alluvial fan, below a gully, registered the maximum accumulation value.
- Period 3/2009–6/2010 (Fig. 3b): a range of values between −1.30 and 1.80 m was selected, despite that the negative values in the deep incision at the foot of the displaced mass were outside that interval (white non-classified area). This range shows a general advance of the lower half of the mass of a value up to 1.30 m, or whatever it might be, a maximum advance of 1.04 m/year (yellowish green to yellow) while in the top of the mass the orthogonal displacements between surfaces indicated an average subsidence of 0.70 m, with a maximum value of 1.20 m, which corresponds to a maximum subsidence rate of 0.96 m/year. (bluish colours).

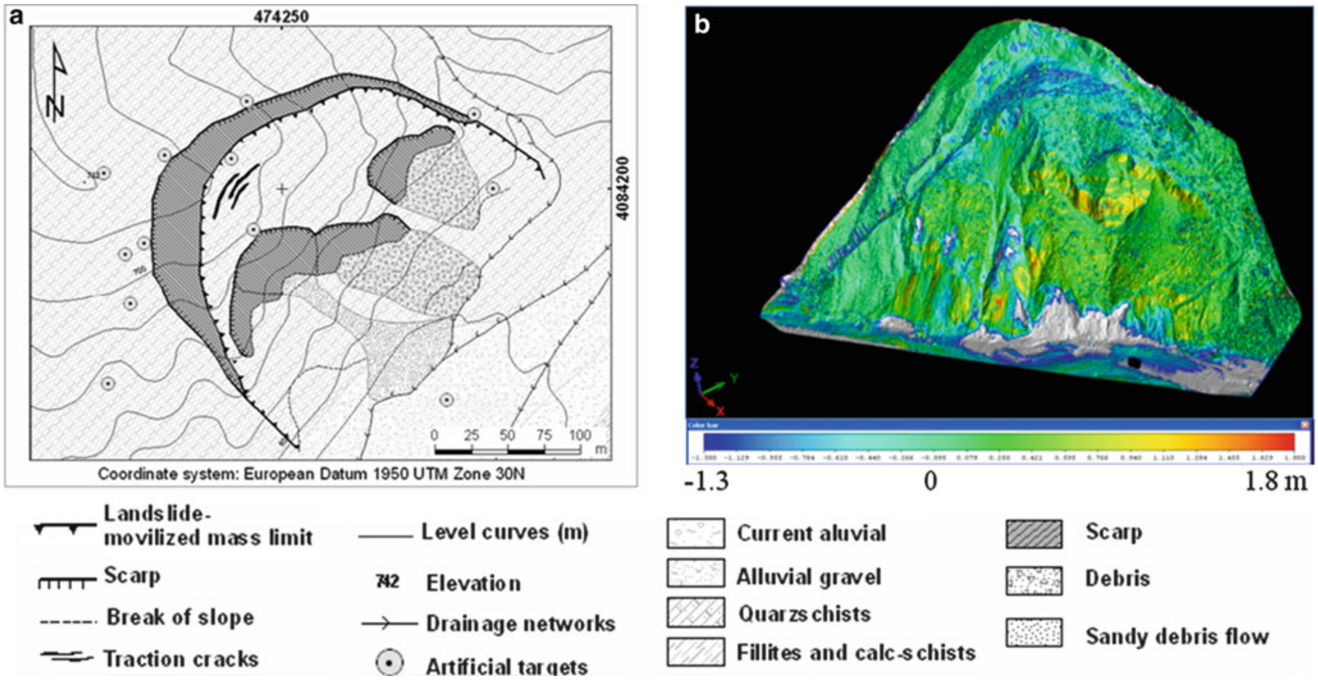

Fig. 3 Almegíjar slide, (**a**) Geomorphological map; (**b**) Classification of orthogonal displacements of the slope surface in March 2010 with regard to its previous position in June 2009, shown in a continuous colour scale

All these results indicate a slide reactivation, with a strain shortening during the last temporal interval similar to a compressive arch-like shape, with its longitudinal length (from bottom to top) shortened, while an advance towards the external part of the displaced mass occurred in the lower half side of the slide (Fig. 4).

Geomorphological Evolution of the Borincho Slide

- Period 3/2009–6/2010: the displacements calculated by comparison of the scanning results of June 2010 and March 2009 range between −3.00 and 0.50 m (Fig. 5b).
- The highest negative values coincide with the collapses affecting the slope mass foot at the border of the River Guadalfeo channel. The area reduction by these collapses has been quantified as 19,345 m^2, with a volume of 49,090 m^3. These features are stored as indirect descriptors useful for assessing the frequency of sliding reactivation based on the amount of reduced mass at the foot of the slide.
- The mass deposits generated during this period are concentrated in zones with a lower slope angle, and in concave zones (small gullies and lower parts of the slide borders in yellowish-green). A neutral zone (white) is established for values between −0.10 and 0.10 m in order to avoid noise produced by changes in vegetation and measuring errors (Fig. 5b).
- Expansion of the scale of negative values in the zone of greatest subsidence located on the right side of the slide foot (Fig. 5a) made it possible to distinguish a zone with values ranging between 8 and 70 cm, composed of semi-elliptical-shaped units interpreted as a set of small incipient planar slides. The zone affected by this subsidence covers 2,610 m^2, with a subsidence rate ranging between 0.32 and 0.56 m/year.

Discussion and Conclusions

The TLS remote monitoring technique has proved to be a rather accurate method for detecting smaller geomorphic features, through the acquisition of slope measurements from scanning positions located about 500 m apart. Thus, this methodology provides information on the temporal evolution of the activity of landslides located in the study area and detects the movement prior to the sudden rupture of the slope without previous access to the displaced mass. The analysis of applying the methodology to these two study areas supports the argument that:

The differential displacements calculated and classified for the Almegíjar slide show that it underwent a reactivation in the period 3/2009–6/2010, and it was in a suspended state between the dates 7/2008 and 3/2009. This reactivation resulted in a slope strain shortening along its longitudinal

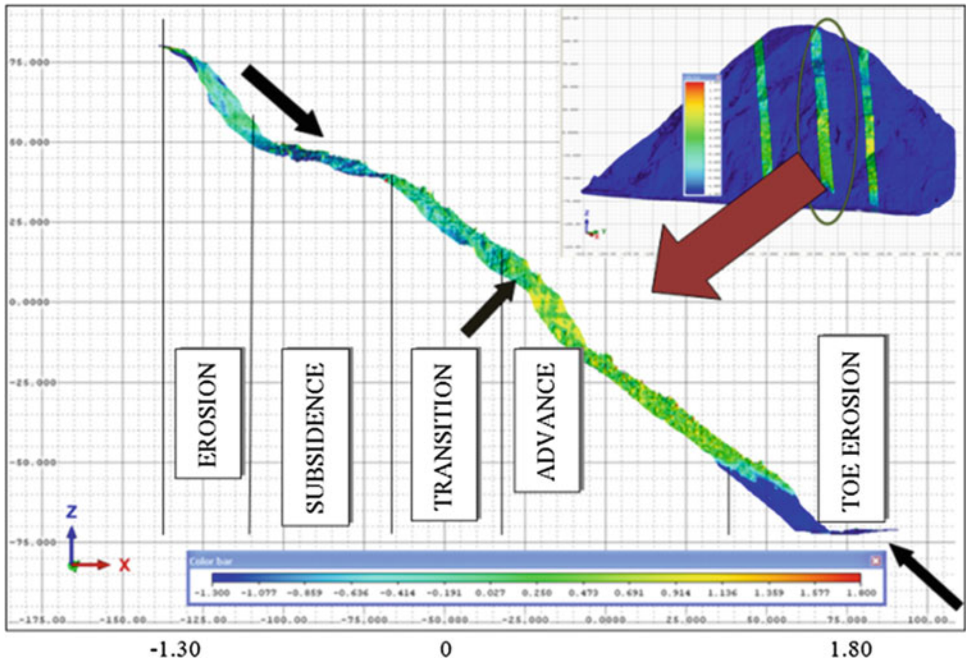

Fig. 4 Lateral view of a metric section in a centred side of the Almegíjar slide showing a classification of displacements between slope surfaces 2010–2009 in the range −1.30 to 1.80 m. From *bottom* to *top* the following processes were observed: erosion-subsidence-transition (very low deformation)-advance-erosion. The *black arrows* indicate the direction of shortening in longitudinal trend, and the extension of the mass perpendicular to the shortening direction

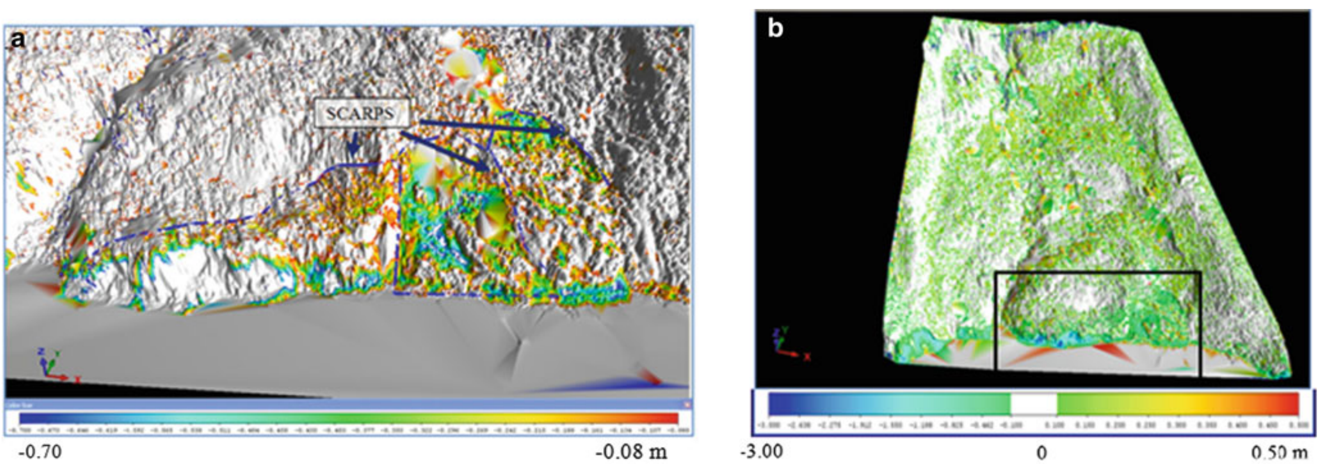

Fig. 5 (**a**) Classification of subsidence zones at the foot of the Borincho slide, shown in Fig. 5b, corresponding to the timing interval March 2009 to June 2010, with enhanced scale in the range −0.70 to −0.08 cm. (**b**) Classification in continuous colour scales of orthogonal displacements in the June 2010 slope surface with regard to the March 2009 slope

axis, and extension perpendicular to this, giving an arch-like shape to the displaced mass.

For the case study of the Borincho slide, a differential slope subsidence located at the foot of the displaced mass in the range from centimeters to decimeters (0.08–0.70 m), associated with 3 new slope ruptures in the incipient to initial stages of activity and semi-elliptical morphology, distinguished by the supervised classification of the displacements measured.

The observed reactivations in both slides coincide with a heavy rainy period between December 2009 and March 2010 (500 mm of rain for this period).

The areas that have undergone a substantial slope alteration in terms of the slide bodies have been mapped digitally and quantified as descriptors of the evolution of the activity of these events, which may be investigated either by techniques of a Geographical Information System (GIS), or by other analytical methods.

Acknowledgements This research was supported by the project CGL200-04854 funded by the Ministry of Science and Innovation of Spain and by the Group RNM 121 of the Andalusian Plan of Research.

References

Abellán A, Calvet J, Vilaplana JM, Blanchard J (2010) Detection and spatial prediction of rockfalls by means of terrestrial laser scanner monitoring. Geomorphology 119(3–4):162–171

Corominas J, Moya J (2008) A review of assessing landslide frequency for hazard zoning purposes. Eng Geol 102(3–4):193–213

Cruden DM, Varnes DJ (1996) Landslide types and processes. Special Report – National Research Council, Transportation Research Board. 247:36–75

Chacón J, Irigaray C, El Hamdouni R, Jiménez-Perálvarez JD (2010) Diachroneity of landslides. Geologically active: proceedings of the 11th IAEG congress. In: Proceedings of the 11th IAEG congress, Auckland, 5-10 Sept 2010, pp 999–1006

Chacón J, Irigaray C, Fernández T, El Hamdouni R (2006) Engineering geology maps: landslides and geographical information systems. Bull Eng Geol Environ 65(4):341–411

Dunning SA, Massey CI, Rosser NJ (2009) Structural and geomorphological features of landslides in the Bhutan Himalaya derived from Terrestrial Laser Scanning. Geomorphology 103(1):17–29

Dunning SA, Rosser NJ, Massey CI (2010) The integration of terrestrial laser scanning and numerical modelling in landslide investigations. Q J Eng Geol Hydrogeol 43(2):233–247

Fell R, Corominas J, Bonnard C, Cascini L, Leroi E, Savage WZ (2008) Guidelines for landslide susceptibility, hazard and risk zoning for land-use planning. Eng Geol 102(3–4):99–111

Fernández P, Irigaray C, Jiménez-Perálvarez J, El Hamdouni R, Crosetto M, Monserrat O, Chacon J (2009) First delimitation of areas affected by ground deformations in the Guadalfeo River Valley and Granada metropolitan area (Spain) using the DInSAR technique. Eng Geol 105(1–2):84–101

Fernández T, Irigaray C, El Hamdouni R, Chacón J (2003) Methodology for landslide susceptibility mapping by means of a GIS. Application to the Contraviesa area (Granada, Spain). Nat Hazards 30(3):297–308

Fernández T, Pérez J L, Delgado J, Cardenal F J, Irigaray C, Chacón J (2011) Evolution of a diachronic landslide by comparison between different DEMs obtained with digital photogrammetry techniques in Las Alpujarras (Granada, Southern Spain). International Symposium on Geo-information for Disaster Management (Gi4DM) Evolution of a diachronic landslide by comparison between different DEMs obtained with digital photogrammetry techniques in Las Alpujarras (Granada, Southern Spain), Antalya, 3–8 Mayo 2011

IAEG (1993) UNESCO Working Party on World Landslide Inventory (WP/WLI). A suggested method for describing the activity of a landslide. Bull Int Assoc Eng Geol París 47(1):453–455

IAEG (1995) UNESCO Working Party on World Landslide Inventory. Working Group on Rate of Movement A suggested method for describing the rate of movement of a landslide. Bull Int Assoc Eng Geol París 47:53–57

Jiménez-Perálvarez JD, Irigaray C, El Hamdouni R, Chacón J (2009) Building models for automatic landslide-susceptibility analysis, mapping and validation in ArcGIS. Nat Hazards 50(3):571–590

Jiménez-Perálvarez JD, Irigaray C, El Hamdouni R, Chacón J (2010) Landslide-susceptibility mapping in a semi-arid mountain environment: an example from the southern slopes of Sierra Nevada (Granada, Spain). Bull Eng Geol Environ. Article in Press (Online First™)

Lichti DD, Jamtsho S (2006) Angular resolution of terrestrial laser scanners. Photogramm Rec 21(114):141–160

Lim M, Petley DN, Rosser NJ, Allison RJ, Long AJ, Pybus D (2005) Combined digital photogrammetry and time-of-flight laser scanning for monitoring cliff evolution. Photogramm Rec 20(110):109–129

Oppikofer T, Jaboyedoff M, Blikra L, Derron MH, Metzger R (2009) Characterization and monitoring of the Åknes rockslide using terrestrial laser scanning. Nat Hazards Ear Syst Sci 9(3):1003–1019

Riegl (2010) Riscan Pro v.1.5.3b10 Operator's manual. Riegl Laser Measurement Systems GmbH, Horn

Riegl (2011) Terrestrial scanning. http://www.riegl.com/nc/products/terrestrial-scanning/produktdetail/product/scanner/4/. Last accessed 8 June 2011

Rosser NJ, Petley DN, Lim M, Dunning SA, Allison RJ (2005) Terrestrial laser scanning for monitoring the process of hard rock coastal cliff erosion. Q J Eng Geol Hydrogeol 38(4):363–375

Teza G, Galgaro A, Zaltron N, Genevois R (2007) Terrestrial laser scanner to detect landslide displacement fields: a new approach. Int J Rem Sens 28(16):3425–3446

Teza G, Pesci A, Genevois R, Galgaro A (2008) Characterization of landslide ground surface kinematics from terrestrial laser scanning and strain field computation. Geomorphology 97(3–4):424–437